RSC Advances

This is an *Accepted Manuscript*, which has been through the Royal Society of Chemistry peer review process and has been accepted for publication.

Accepted Manuscripts are published online shortly after acceptance, before technical editing, formatting and proof reading. Using this free service, authors can make their results available to the community, in citable form, before we publish the edited article. This *Accepted Manuscript* will be replaced by the edited, formatted and paginated article as soon as this is available.

You can find more information about *Accepted Manuscripts* in the **Information for Authors**.

Please note that technical editing may introduce minor changes to the text and/or graphics, which may alter content. The journal's standard **Terms & Conditions** and the **Ethical guidelines** still apply. In no event shall the Royal Society of Chemistry be held responsible for any errors or omissions in this *Accepted Manuscript* or any consequences arising from the use of any information it contains.

www.rsc.org/advances

A Free Radical Assisted Strategy for Preparing Functionalized Carbon Nanotubes as a Highly Efficient Nucleating Agent for Poly(L-lactide)

Zi-Jing Zhang, Wei Cui, Huan Xu, Lan Xie, Huan Liu, Le-Min Zhu, Hang Li, Rong Ran*
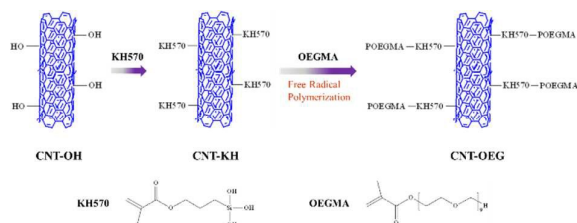
Schematic illumination of the fabrication of the CNT-OEG *via* free radical polymerization.

1 **A Free Radical Assisted Strategy for Preparing**

2 **FunctionalizedCarbon Nanotubes as a Highly Efficient**

3 **Nucleating Agent for Poly(L-lactide)**

4 Zi-Jing Zhang, Wei Cui, Huan Xu, Lan Xie, Huan Liu,Le-Min Zhu,Hang Li,Rong Ran*

5 *College of Polymer Science and Engineering, State Key Laboratory of Polymer Materials*

6 *Engineering, Sichuan University, Chengdu 610065, China*

7 **Abstract**

8 In this work, we synthesized novel functionalized carbon nanotubes (CNTs) by

9 grafting poly(ethylene glycol) methyl ether methacrylate (OEGMA) onto CNTs *via*

10 free radical polymerization in which the 3-methacryloxypropyltrimethoxysilane

11 (KH570)was used as the silane coupling agent. The resulting OEGMA grafted CNTs

12 (CNT-OEG) were systematically characterized by fourier transform infrared

13 spectroscopy (FTIR), thermal analysis, transmission electron microscope (TEM) and

14 X-ray photoelectron spectroscopy (XPS).Then the obtained CNT-OEG was added to

15 PLA as a crystallization nucleation agent. The crystallization behavior of the

16 CNT-OEG/PLA composites was investigated under isothermal and nonisothermal

17 conditions using differential scanning calorimeter (DSC) and polarized optical

18 microscopy (POM). Interestingly, our results suggested that the addition of CNT-OEG

19 improve the crystallization rate of PLA dramatically. Besides, the decoration of CNTs

20 *via* free radical polymerization facilitate their distribution in the matrix. This robust

21 method to connect reactive polymers to nanofillers including, but not limited to,

22 graphene, clay and cellulose nanofibrils, may significantly facilitate their utilized in

23 traditional composites or biological engineering materials.

24 **Keywords:** Carbon nanotubes; Free radical polymerization; Poly($_L$-lactide);

25 Nanocomposite.

Introduction

27 Carbon nanotubes (CNTs) have been regarded as promising nanofillers in polymer

28 nanocomposites owing to their excellent properties, such as high mechanical strength,

29 electrical and thermal conductivity, along with high aspect ratios and small sizes.[1-3]

30 The existing literatures show that besides the nanofillers role, CNTs can also act as

31 efficient nucleating agents for polymers and affect their crystallization kinetics and

32 crystalline morphology.[4] Therefore, various semicrystalline polymers, such as

33 poly(lactic acid) (PLA),[5] isotactic polypropylene (iPP),[6]

34 poly(3-hydroxybutyrate-co-3-hydroxyvalerate) (PHBV)[7], and polyamide (PA),[8] have

35 been compounded with CNTs in order to improve their crystallization behavior.

36 Among them, PLA has been attracting much attention because of its excellent

37 biodegradability, biocompatibility, renewability, and mechanical properties.[9]

38 Unfortunately, owing to its intrinsic slow crystallization rate, PLA products are

39 usually amorphous, especially under conventional processing conditions such as

40 injection molding and extrusion, leading to some undesirable results such as

41 decreased of barrier property and thermal resistance. A much number of approaches

42 have been proposed in an endeavor to facilitating the crystallization rate of PLA. The

43 addition of CNTs is one of the most effective methods.[10] It has been reported that only

44 0.02 wt% multiwalled carbon nanotubes (MW-CNTs) could reduce the

45   half-crystallization time ($t_{1/2}$) of PLA from 23 min to 5.5 min when isothermally

46   crystallized at 115 °C, which may finally result in its improvement in physical and

47   mechanical properties.[11]

48   Recent studies indicated that the surface functional groups on CNTs had a strong

49   influence on the crystallization of polymer nanocomposites.[12, 13]CNTs with proper

50   functional groups facilitate the dispersion and interfacial adhesion with polymer

51   matrix which will further boost the crystallization of polymer matrix.[14] Thus,

52   surface-functionalization of CNTs with covalent grafting of organic compound or

53   polymer were employed to improve properties of CNTs such as solubility, interfacial

54   interactivity with a target matrix, and obtained good mechanical properties

55   composites. There are several methods for covalent grafting of polymers, including

56   "grafting from" and "grafting onto" methods.[15, 16] The "grafting onto" method leads to

57   low grafting density at the surface of CNTs, due to significant steric hindrances when

58   polymeric chains diffuse to the surface of CNTs. Whilst, the advantage of "grafting

59   from" techniques over "grafting onto" techniques is to give access to high-dense and

60   controllable polymer-grafted CNTs. Based on merits of "grafting from" techniques, a

61   number of composites of nanoparticles with polymers have been prepared *via* several

62   polymerization methods, such as free radical polymerization, living radical

63   polymerization, ring-opening polymerization and cationic/anionic polymerization.[1]

64   Among them, free radical polymerization is one of the robust methods for preparation

65   of polymer-based nanocomposites attributing to its abundance of monomer and mild

66   reaction conditions.[17] Recently, Saeid Rahimi-Razin et. al.[18] developed a novel method

67 to synthesize polymerizable multiwalled carbon nanotubes through the silanization

68 reaction of a methyl methacrylate containing silane agents with hydroxylated

69 MWCNTs. On the basis of this work, we fabricate polymerizable CNTs using silane

70 coupling agent which carries an silane group reserved for the reaction with CNTs and

71 a vinyl group for subsequent free radical polymerization. However there comes

72 another interesting issue: what kind of polymer chains should we choose to decorate

73 the CNTs in order to improve the crystallization property of polymer matrix?

74   Recently, some reports have been published, which results show that plasticizers

75 such as poly(ethylene glycol) (PEG), glucose monoesters and partial fatty acid esters

76 could be used to improve the flexibility of PLA.[19, 20]Among them PEG is polar,

77 water-soluble, good biocompatible and miscible with PLA, so it has been wildly used

78 in PLA matrix in recent decades.[21, 22] Moreover, PEG chains can increase the polymer

79 chain mobility, which leads to an enhancement in the crystallization of PLA via a

80 reduction in the energy required for the chain folding process during crystallization.[23,

81 [24]Yang et al. has mentioned that the crystallization behavior of PLA could be

82 influenced by the addition ofPEG.[25] In PEG/PLA blend systems, PEG promoted the

83 spherulite growth rate but depressed the nucleation density of PLA. It has been

84 reported that the existence of PEG not only facilitated the growth rates of trans

85 crystallinity but also improved the preferential orientation of PLAchains.[26] Based on

86 their works, we choose OEGMA, containing PEG chains as well as a vinyl group, as a

87 candidate to decorate CNTs.

88   In our previous research[27] we proposed a method to synthesize a type of

89   nanoparticle with the functionalized nanofiller in the polymer matrix by using

90   glycidyl methacrylate (GMA), which carries an epoxy group reserved for the reaction

91   with nanotitania and a vinyl group for subsequent RAFT polymerization. In this study,

92   we explored a strategy to prepare CNT/PLA nanocomposites with significantly

93   modified crystallization behavior using CNT-OEG. The nucleation ability of CNTs

94   was improved efficiently by grafting PLA-miscible polymer chains onto the CNTs

95   surfaces. Simultaneously, PEG side chains of OEGMA can act as a plasticizer and

96   improve the chain mobility of PLA during the process of spherulite growth. The

97   results show us an efficient way to improve the dispersion and interfacial interactions

98   between CNT and semicrystalline polymers through a simple and general free radical

99   polymerization reaction.

100

Experimental Section

101

102 **Materials**

103   Commercially available PLA comprising 2% DLA (trade name 4032D) was

104 manufactured by Nature Works LLC (USA). The weight-average molecular weight

105 and number-average molecular weight of PLA were 2.23×10^5 and 1.06×10^5 g/mol,

106 respectively. The CNTs and hydroxyl CNTs (CNT-OH) with ~30 μm length and 20-30

107 nm diameter were purchased from Chengdu Organic Chemicals Co Ltd, the Chinese

108 Academy of Sciences R&D center for Carbon Nanotubes. The weight ratio of -OH

109 group in CNT-OH is about 1.76 wt%. 3-methacryloxypropyltrimethoxysilane (KH570)

110 and OEGMA (the average number molecular weight (Mn) of OEGMA is 475) were

111   acquired from J&K Scientific Co. (Guangdong, China). All other reagents were

112   purchased from Kelong Chemical Co. (Chengdu, China) and used as received.

Synthesis of KH570-modified CNT (CNT-KH)

114   The fabrication of CNT-OEG mainly contains two procedures (as shown in Figure

115   1). (I) The introduction of double bonds to CNT via KH570. (II) The attachment of

116   OEGMA to CNT-KH *via* free radical polymerization. The detailed synthesis process

117   of CNT-KH was as follows: CNT-OH (100 mg) were dispersed in 100 mL deionized

118   water and the suspension was treated with ultrasound for 30 min, yielding completely

119   exfoliated CNT-OH suspension. Then, KH570 was added into the as-prepared liquid

120   and the reaction solution was adjusted to a pH value of 4.5. The hydrolysis of KH570

121   and condensation of CNT-OH were carried out simultaneously at 60 °C for 12 h to

122   produce the KH570 functionalized CNTs solution. The methoxy groups of KH570

123   hydrolyze readily in aqueous solvents to form silanol groups, and self-condensation of

124   the silanol to insoluble polysiloxane was likely to occur, greatly hindering the

125   condensation between the silanol groups and the hydroxyl groups on the CNT-OH.

126   Thus, the experimental condition(pH 4.5) facilitated the hydrolysis reaction while

127   restrained the self-condensation reaction to ensure that a majority of silanol groups

128   sufficiently condensed with hydroxyl groups on the CNT-OH.[28, 29]The KH570

129   modified CNTs (CNT-KH) were obtained by centrifugation and redispersion in water

130   for 4 times. The deposit was dried to constant weight at 60 °C in vacuum for 24 h.

Synthesis of CNT-OEG *via* free radical polymerization

132   The CNT-KH obtained above was dissolved into dioxane with ultrasound for 30

133 min, then 5g OEGMA, 0.02g AIBN and 0.01 g divinylbenzene (DVB) were added

134 into the solution as illustrated in Figure 1. Incorporation of a very small amount of

135 DVB led to the emergence of branched and starlike chains without gelation,

136 effectively increasing grafting rate of OEGMA onto the CNTs.[30, 31]The mixture was

137 reacted at 70 °C for 12 h under N_2 atmosphere, centrifugation and redispersion in

138 water and ethanol for 3 times. Finally, the resulting product was dried at 40 °C under

139 vacuum for further use. The obtained product was CNT-OEG.

140
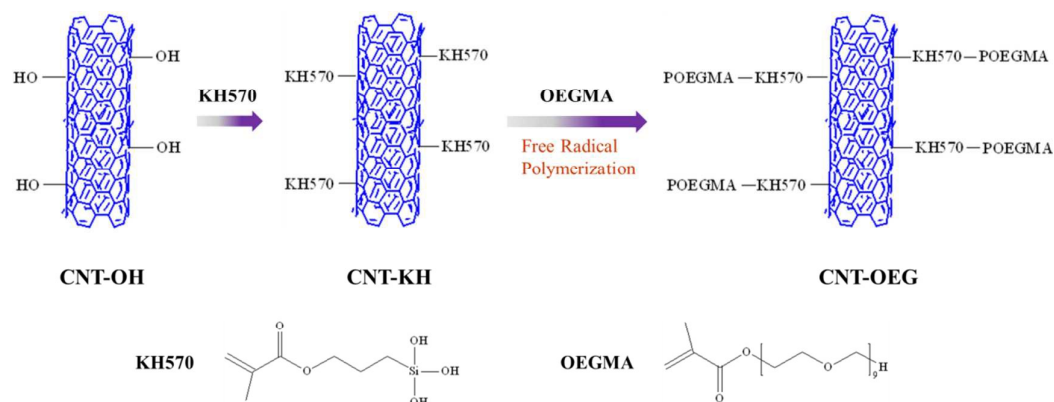
141 **Figure 1.** Schematic illumination of the fabrication of the CNT-OEG *via* free radical

142 polymerization.

143 **Preparation of PLA/CNT-OEG nanocomposites**

144 Solution coagulation method was utilized to guarantee the good distribution of

145 CNT nanofillers in PLA. Taking PLA/CNT-OEG (100:0.1 wt/wt) as an example, the

146 detailed procedure was as follows: 0.01 g of CNT-OEG was added to 100 mL of

147 ethanol (C_2H_5OH), then the mixture was subjected to ultrasound for 60 min to obtain

148 a uniform dispersion. 10 g of PLA was completely dissolved in 100 mL of

149 dichloromethane (CH_2Cl_2), subsequently. By pouring the predispersed

150 C_2H_5OH/CNT-OEG suspension into the CH_2Cl_2/PLA hybrid, coagulated material

151   precipitated continuously. The PLA/CNT-OEG coagulates were then transferred to

152   blowing dryer，left overnight at 55 °C, and dried in a vacuum oven for 24 h at 80 °C

153   to remove residual solvent. PLA/CNT and PLA/CNT-OH were also prepared using

154   the same method.

155   **Characterization**

156   TEM images were taken on a JEOL-100CX transmission electron microscope (JEOL,

157   Japan) to examine the morphology of the CNT-OH and CNT-OEG samples. The

158   samples were prepared by one drop casting on a lacy copper grid followed by

159   evaporation of the solvent at room temperature. XPS experiments were carried out on

160   an XSAM800 (Kratos Company, UK) with Al Kα radiation (hυ = 1486.6 eV). In order

161   to determine the successful fabrication of CNT-OEG, FTIR spectra were recorded

162   with Nioclent 6700 spectrophotometer (Thermal Scientific, USA)within the range

163   400–4000 cm^{-1} using a resolution of 0.5 cm^{-1}. All spectra were baseline corrected.

164   Thermal gravimetric analysis (TGA) was carried out under a nitrogen atmosphere on

165   a Netzsch TG 209 F1 apparatus using a heating rate of 10 °C/min from 40 to 800°C.

166   Gel permeation chromatography (GPC) analysis was performed at 40°C on a

167   HLC-8320GPC system (Dong Chao corporation, Japan), equipped with two columns

168   (Column Super HM-H, 6.0mm×15cm), and a differential refractive-index detector.

169   POM observation was performed on an Olympus BX51 polarizing optical microscopy

170   (Olympus Co., Tokyo, Japan) equipped with a Micro Publisher 3.3 RTV CCD. The

171   temperature was controlled by a Linkam CSS-450 high temperature optical stage. The

172   samples were first heated to 190 °C at a rate of 30°C/min and held at this temperature

173   for 5 min to eliminate thermal history. Then cooled to 130 °C at cooling rates of 30 °C

174   /min and held for 30 min. DSC measurements were carried out in a TA-Q200 DSC

175   (TA Instruments, USA) under a nitrogen flow, and calibrated by indium as the

176   standard. For nonisothermal crystallization, samples were first heated to 190 °C at a

177   rate of 10 °C /min and held at 190 °C for 3 min to erase thermal history. Then, they

178   were cooled to 40 °C at cooling rates of 5 °C /min and reheated at a rate of 10 °C /min.

179   For isothermal crystallization, the samples were also first annealed at 190 °C for 3

180   min to eliminate any thermal history and then quenched at a rate of 30 °C /min to the

181   desired isothermal crystallization temperatures (T_c) (120 °C, 125 °C and 130 °C) for

182   30 min. The degree of crystallinity (X_r) during heating progress is calculated using the

183   equation: $X_r = 100 \times (\Delta H_{cc} + \Delta H_m)/\Delta H_0$, in which the heat of melting of perfectly

184   crystalline PLA (ΔH_0) was 93.0 J/g. ΔH_{cc} was the cold crystalline enthalpy; ΔH_m was

185   the melt enthalpy.[32]

186

187

188   **Results and discussion**

189   **Characterization ofCNT-OEG**

190   The morphology of CNT-OH and CNT-OEG was examined by TEM. Figure 2

191   shows their TEM images. An enlarged diameter of CNT-OEG samples compared to

192   CNT-OH which may results from the covered poly(OEGMA) (POEGMA) layers was

193   observed clearly.[33]As a silane coupling agent, KH570 can chemically link to CNT-OH

194   *via* reactive groups(Si-O-CH$_3$) react with the hydroxy groups of CNT-OH. Then the

195   KH570 bonded to the CNT surface was copolymerized with OEGMA *via* a radical

196   polymerization to form CNT-OEG. Similar results have been reported by Tang et al.[34]

197   They claimed that the enlarged diameter of modified CNT samples is consistent with

198   the chemical-linked polymer on the surface of CNTs.

199
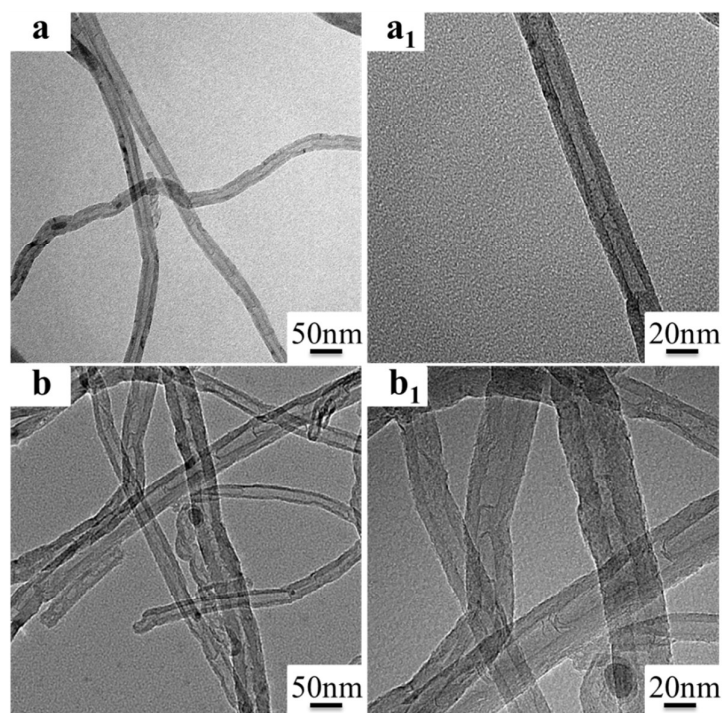
200

201   **Figure 2.** TEM images of the CNT-OH (a,a$_1$) and CNT-OEG (b,b$_1$).

202   XPS was employed to further determine the presence of POEGMA moieties on the

203   surfaces of the CNT-OEG. As shown in Figure 3, the peaks at 530.6, 258.5, 102.5 and

204   156.5 eV in the full spectrum of CNT-OEG are assigned to O, C, Si 2p and Si 2s

205   elements (Figure3a), respectively. Compared with CNT-OH, the appearance of Si 2p

206   band in the spectrum of CNT-OEG originates from the covalent attachment of

207   OEGMA on the edges of CNT-OEG.[18, 35] The change in C, O and Si contents

208   calculated from the XPS results further confirms the introduction of KH570 and

209　OEGMA atoms, as listed in Table 1. These results also demonstrated that OEGMA

210　moieties were successfully anchored onto the surface of CNTs.
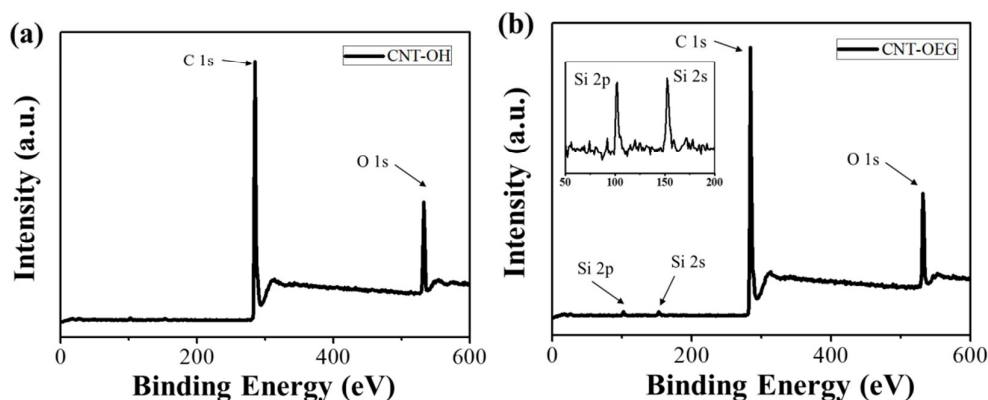
211

212　**Figure 3.** XPS spectra for CNT-OH (a) and CNT-OEG (b).

213　**Table 1.** Summary of the element composition of the CNT-OH and CNT-OEG

Element (Atom %)	C	O	Si
CNT-OH	91.9	8.1	—
CNT-OEG	86.9	11.8	1.4

214

215　Figure 4 shows the FTIR spectra of the CNT-OH (curve a), the CNT-KH (curve b)

216　and the CNT-OEG (curve c). The strong absorption peaks at 1620 cm^{-1} is assigned to

217　C=C stretching mode of sp^2 network of CNT basal plane which can be seen in all

218　these three samples.[36] The broad absorption at 3300–3400 cm^{-1} is the stretching

219　vibration of the -OH groups on the CNT-OH surface.[37] Compared with the FTIR

220　spectra of CNT-OH, the FTIR spectra of CNT-KH and CNT-OEG show the

221　characteristic absorption of CNT-OH at 1620 cm^{-1}，and the increasing intensity of

222　absorption at 3300–3400 cm^{-1}, stemming from the reason that there have much more

223   -OH groups in both KH570 and POEGMA. With comparison of FTIR spectra of

224   CNT-KH, CNT-OEG reveals that the intensities of the bands at 1711cm^{-1} (stretching

225   vibration of C=O)[38], 2860 cm^{-1} and 2930 cm^{-1} (symmetric and asymmetric vibration

226   of -CH$_2$) have increased significantly after the free radical polymerization. Moreover,

227   the appearance of band at 1091 cm^{-1} (Si–O–C/Si–O–Si) provided more evidence for

228   this successful chemical functionalization.[39] The FTIR spectrum confirms that the

229   POEGMA molecules are covalently bound to the CNT-OH, as represented in Scheme

230   1.
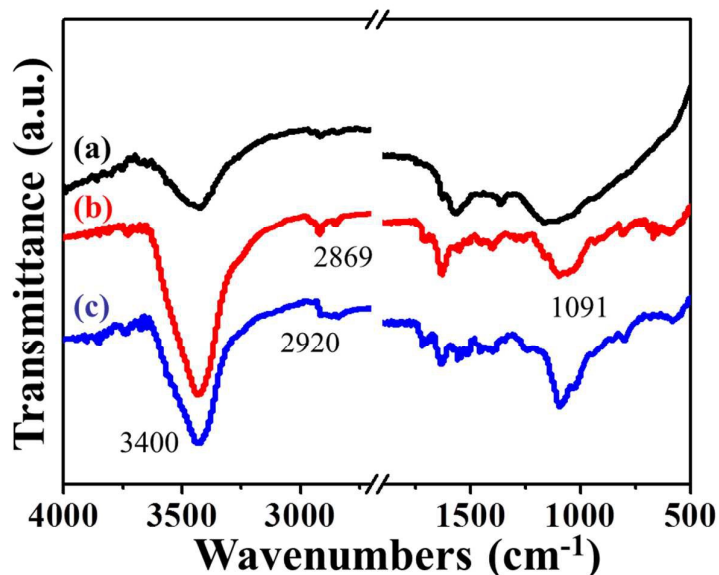
231

232   **Figure 4.** FTIR spectra of CNT-OH (a), CNT-KH (b), and CNT-OEG(c).

233   Further evidence for the fabrication of CNT-OEG can be ascertained from TGA

234   measurement. Figure 5 shows that the thermal degradation of CNT-OH, CNT-KH and

235   CNT-OEG occurs in stages during heating from 40 ℃ to 800 ℃ under N$_2$ atmosphere.

236   As shown in Figure 5a, 5.2% of mass loss is resulted from pyrolysis of the unstable

237   functionalized -OH groups in CNT-OH. Obviously, the major mass loss of CNT-OEG

238 occurs between 300-400 ℃，which is mainly corresponded to the pyrolysis of the

239 grafted POEGMA on CNTs. Taking into account the residue of CNT-OEG and

240 CNT-KH at 800 ℃, the grafting ratio of POEGMA is estimated as 9 wt%. Therefore,

241 the grafting ratio by this method is efficient to change the characterization of the

242 CNTs as well as their nanocomposites.
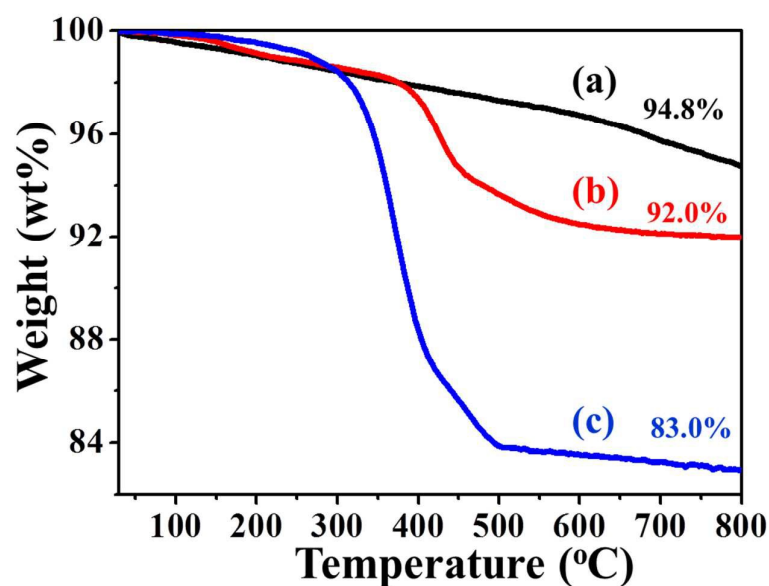
243

244 **Figure5.** TGA curves of CNT-OH (a) CNT-KH (b) and CNT-OEG (c).

245 The existing literatures show that polymerization both in solution and on the

246 surface of CNT-OEG was not differ significantly, the molecular weights and

247 polydispersity index (*PDI*) of the POEMGA formed both in solution and on the

248 surface of CNT-OEG were almost same.[40] Herein, the molecular weight of the

249 POEMGA on the surface of CNT-OEG could be estimated by the molecular weight of

250 the POEGMA formed in solution. Figure 6, shows the GPC trace of the POEMGA

251 recovered in solution. The *Mn* of POEGMA is about 9190 and the *PDI* is 1.48.

Elution time (min)
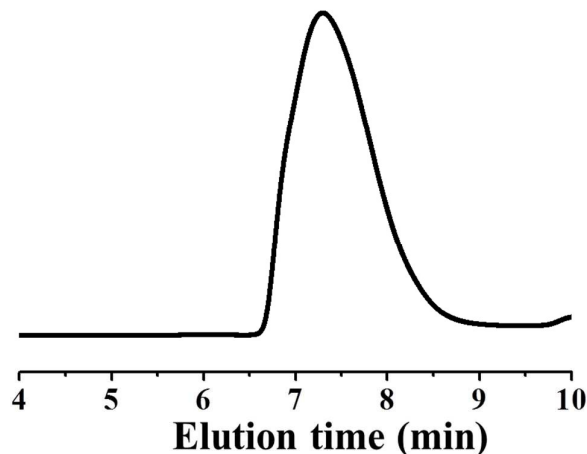
252

253 **Figure 6.**GPC traces of free POEGMA recovered from polymerization solution. The *Mn* of

254 POEGMA is 9190. The *PDI*=1.48.

255 **Crystallization kinetics of PLA/CNT-OEG nanocomposites**

256 The isothermal crystallization performances of PLA/CNT-OEG composites were

257 firstly investigated by POM with the filler weight ratio of 0.1 wt%. The PLA/CNT,

258 PLA/CNT-OH composites with the same weight ratio were also prepared for

259 comparison. As shown in Figure 7, compared to the PLA/CNT, the observation of

260 remarkably decreased density of spherulites after adding CNT-OH can be illustrated

261 by the weak interfacial interaction and the steric effect between the PLA and

262 CNT-OH.[41] What arouse our interests is that the density of spherulites rises

263 considerably for PLA/CNT-OEG. Fujisawa et al. results show us that enhancing

264 dispersion, crystallization kinetics, and interfacial interaction within PLA matrix can

265 be obtained when cellulose nanofibrils are decorated with PEG chains.[42, 43] Therefore,

266 we believe that the dispersion of CNT-OEG is improved and some attractive

267 interactions are likely to be formed between the PEG side chain of POEGMA on the

268 surface of CNT-OEG and PLA matrix. It was these enhancing dispersion and

269   attractive interactions that enhanced the crystallization kinetics of PLA effectively.
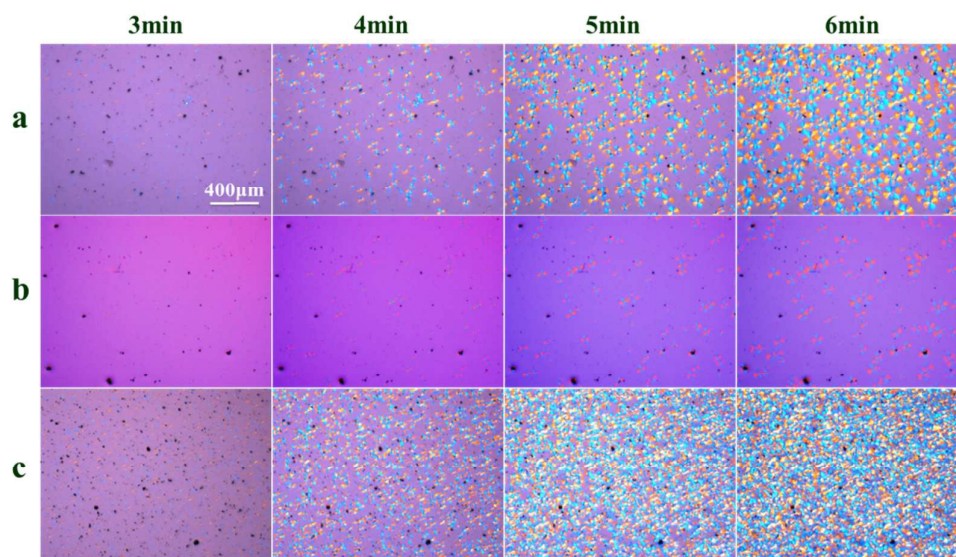
271   **Figure7.**POM of PLA and PLA/CNT nanocomposites during isothermally crystallizing at

272   130 °C: (a) PLA/CNT, (b) PLA/CNT-OH, (c) PLA/CNT-OEG.

273   Figure 8A shows the relative crystallinity ($X(t)$) derived from the DSC isothermal

274   crystallized as a function of the crystallization time for the PLA nanocomposites

275   isothermally crystallized at 120 °C. All these curves have similar sigmoid shapes,

276   moreover, the corresponding crystallization time for PLA/CNT-OH is much shorter

277   than that of PLA/CNT. What arouse our interest is that the time to complete the

278   crystallization of PLA is markedly reduced by the incorporation of CNT-OEG. It is

279   obvious that the incorporation of the POEGMA chains enhance the isothermal

280   crystallization of PLA remarkably when compared with untreated CNTs. The half

281   crystallization time ($t_{1/2}$) derived from the DSC isothermal crystallized at different

282   temperatures are displayed in Figure 8B. The crystallization rate ($1/t_{1/2}$) of the

283   PLA/CNT-OEG is vitally boosted at each temperature. For instance, the $t_{1/2}$ of

284   PLA/CNT, PLA/CNT-OH is 14.6 min, 10.3 min at 125 °C respectively. With addition

285   of 0.1 wt% CNT-OEG, an unprecedented 5.5 min reduce of $t_{1/2}$ can be obtained. As

286   temperature increases ranging from 120 °C to 125 °C, the $t_{1/2}$ increases as well for

287   PLA/CNT and PLA/CNT-OH composites. It is acknowledged that the formation of

288   polymeric spherulite is essentially dependent on nucleation and crystal growth. It

289   results from a compromise between nucleation and growth of crystals: crystal

290   nucleation is favored at low temperature when molecular mobility is low, whereas

291   crystal growth is favored at high temperature when viscosity is low.[10, 44, 45] Beyond

292   110 °C, the nucleation is blocked due to the low viscosity of polymer chains, so the

293    $t_{1/2}$ increases   linearly.   In   contrast   to   PLA/CNT   and   PLA/CNT-OH,   the

294   PLA/CNT-OEG sample exhibits limited change with temperatures. It stems from the

295   superb nucleation ability of CNT-OEG. Thus we can conclude that effect of the access

296   crystallization ability of PLA is CNT-OEG>CNT-OH>CNT.

297

298
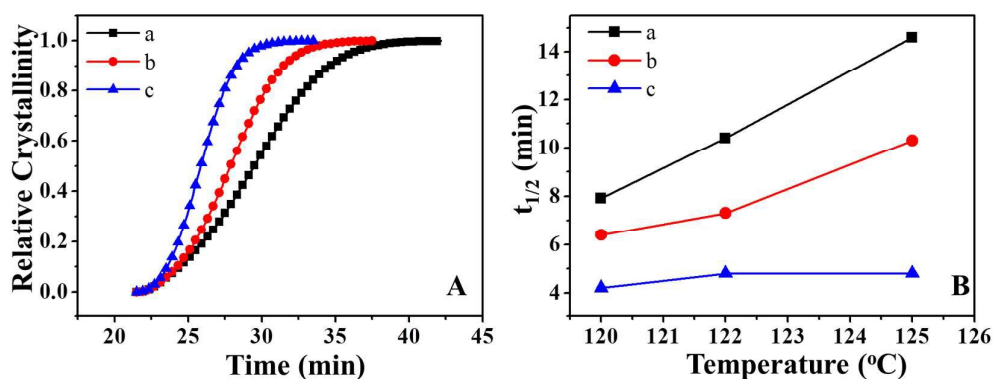
299

300   **Figure8.** (A) Plots of *X(t)* *versus* the crystallization time for the composites crystallized

301   isothermally at 120 °C and (B) the plot of $t_{1/2}$ of the composites crystallized isothermally *versus*

302   temperature: (a) PLA/CNT, (b) PLA/CNT-OH, (c) PLA/CNT-OEG.

303   Figure 9A shows the cooling DSC curves of PLA composites after eliminating their

304   thermal history. The crystallization peak temperature (T_p) of PLA/CNT-OH and

305   PLA/CNT are faintly detectable compared to PLA/CNT-OEG, confirming the strong

306   nucleating ability of CNT-OEG.[46] Compared with T_p and crystallization enthalpy (H_c)

307   of PLA/CNT and PLA/CNT-OH，the increasing of T_p and H_c of PLA/CNT-OEG

308   indicates that the functional groups affects the nucleation ability of CNT. The DSC

309   traces in the second heating run (Figure 9B) evidences a strong cold crystallization

310   peak of PLA/CNT and PLA/CNT-OH. On the contrary, the cold crystallization peak

311   of nanocomposites PLA/CNT-OEG almost disappeared. The result suggesting that the

312   strong interactions at the polymer-filler interface promotes the crystallization process

313   of PLA. Similar conclusions have been reported by Mariano Pracella et al.[47] for

314   composites containing cellulose nanofibres and PVAc. The Xr of PLA

315   nanocomposites are listed in Table2. The Xr of PLA/CNT and PLA/CNT-OH are 9.2 %

316   and 11.8 % respectively, while the Xr of PLA/CNT-OEG is 32.8 %. In PLA/CNT, the

317   CNTs were suggested to provide the templates for PLA chains to landscape. In

318   PLA/CNT-OEG, the presence of POEGMA may facilitate the dispersion of

319   CNT-OEG in matrix. Thus more nuclei spots were obtained. Furthermore, POEGMA

320   chains can also act as crystal accelerator, so the growth of crystal is boosted. The

321   synergistic effect of nucleation and growth of CNT-OEG on the PLA crystallization

322   give rise to the enhancement on the overall crystallization kinetics of PLA as shown in

323   DSC results. Furthermore, the high crystallinity of PLA/CNT-OEG nanocomposites

324   will be benefit to improve the properties of PLA products, thus widening their

325   application fields.[48]

326
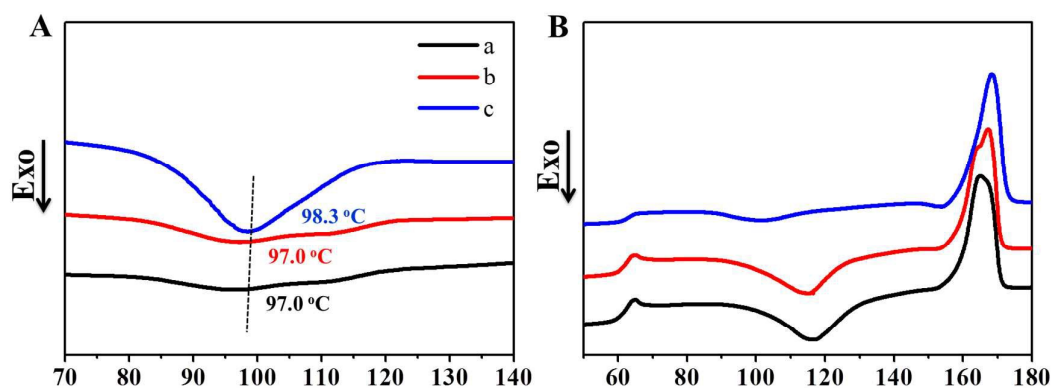
327

328   **Figure9.** Nonisothermal DSC scans of PLA nanocmposites at a constant cooling rate of 5

329   ℃/min (A), and its heating curves at a constant heating rate of 10 ℃/min (B): (a) PLA/CNT, (b)

330   PLA/CNT-OH, (c) PLA/CNT-OEG.

331

332   **Table 2.** The cold crystallization peak (T_{cc}), exothermic heat of cold crystallization (H_{cc}),

333   melting temperature (T_m), endothermic heat of melting (H_m) and crystallinity (X_r) of PLA

334   nanocomposites obtained from the heating scan.

Samples	T_{cc}	H_{cc}	T_m	H_m	$X_r(\%)$
PLA/CNT	117.0	24.2	165.0	32.8	9.2
PLA/CNT-OH	116.1	21.7	167.3	32.7	11.8
PLA/CNT-OEG	102.1	8.0	168.5	38.5	32.8

335

336

337   **Conclusion**

338   In the present work, we have demonstrated a simple way to fabricated CNT-OEG *via*

339 free radical polymerization by using silane coupling agents. The structure of

340 CNT-OEG was confirmed by FTIR, TEM, XPS and TGA. Effects of CNT-OEG on

341 the crystallization of PLA were studied through DSC and POM. The addition of

342 CNT-OEG to PLA matrix significantly increased the crystallization rate of PLA. The

343 POEGMA chains immobilized on the surface of the CNT may accelerate nucleation

344 rate of PLA. Therefore the CNT-OEG is expected to be used as an effective nucleating

345 agent for semicrystalline biopolymers. It is worth stressing that this chemical

346 methodology to graft polymers on the surface of CNTs explored herein is simple and

347 has the potential to allow better integration of CNTs into multicomponent systems.

348 The results shown here could have wide implications since they demonstrate that it is

349 possible to use a simple and general chemical reaction to connect reactive polymers

350 like PS, PMMA, PVA, etc. and CNTs with very different but complementary

351 properties.

360 **Reference**

361 1.   Z. Spitalsky, D. Tasis, K. Papagelis and C. Galiotis, *Progress in Polymer Science*, 2010, **35**,
362   357-401.
363 2.   T. Dürkop, B. Kim and M. Fuhrer, *Journal of Physics: Condensed Matter*, 2004, **16**, R553.

364   3.   J. Hone, *Dekker Encyclopedia of Nanoscience and Nanotechnology, Marcel Dekker, Inc., New*
365   *York*, 2004, 603-610.

366   4.   N. Ning, S. Fu, W. Zhang, F. Chen, K. Wang, H. Deng, Q. Zhang and Q. Fu, *Progress in*
367   *Polymer Science*, 2012, **37**, 1425-1455.

368   5.   C.-F. Kuan, H.-C. Kuan, C.-C. M. Ma and C.-H. Chen, *Journal of Physics and Chemistry of*
369   *Solids*, 2008, **69**, 1395-1398.

370   6.   M. Haque, M. Mina, A. Moshiul Alam, M. Rahman, M. Bhuiyan, A. Hashan and T. Asano,
371   *Polymer Composites*, 2012, **33**, 1094-1104.

372   7.   E. Ten, J. Turtle, D. Bahr, L. Jiang and M. Wolcott, *Polymer*, 2010, **51**, 2652-2660.

373   8.   S. Chatterjee, F. Nüesch and B. T. Chu, *Nanotechnology*, 2011, **22**, 275714.

374   9.   A. J. Lasprilla, G. A. Martinez, B. H. Lunelli and A. L. Jardini, *Biotechnology advances*, 2012,
375   **30**, 321-328.

376   10.   S. Barrau, C. Vanmansart, M. Moreau, A. Addad, G. Stoclet, J.-M. Lefebvre and R. Seguela,
377   *Macromolecules*, 2011, **44**, 6496-6502.

378   11.   H.-S. Xu, X. J. Dai, P. R. Lamb and Z.-M. Li, *Journal of Polymer Science Part B: Polymer*
379   *Physics*, 2009, **47**, 2341-2352.

380   12.   X. Hu, H. An, Z.-M. Li, Y. Geng, L. Li and C. Yang, *Macromolecules*, 2009, **42**, 3215-3218.

381   13.   J.-Z. Xu, G.-J. Zhong, B. S. Hsiao, Q. Fu and Z.-M. Li, *Progress in Polymer Science*, 2014, **39**,
382   555-593.

383   14.   W. Li, Z. Xu, L. Chen, M. Shan, X. Tian, C. Yang, H. Lv and X. Qian, *Chemical Engineering*
384   *Journal*, 2014, **237**, 291-299.

385   15.   H. Roghani-Mamaqani, V. Haddadi-Asl and M. Salami-Kalajahi, *Polymer Reviews*, 2012, **52**,
386   142-188.

387   16.   C. M. Homenick, G. Lawson and A. Adronov, *Polymer Reviews*, 2007, **47**, 265-290.

388   17.   H. Peng, L. B. Alemany, J. L. Margrave and V. N. Khabashesku, *Journal of the American*
389   *Chemical Society*, 2003, **125**, 15174-15182.

390   18.   S. Rahimi‑Razin, V. Haddadi‑Asl, M. Salami‑Kalajahi, F. Behboodi‑Sadabad and H.
391   Roghani‑Mamaqani, *International Journal of Chemical Kinetics*, 2012, **44**, 555-569.

392   19.   A. S. Hoffman, *Advanced Drug Delivery Reviews*, 2002, **54**, 3-12.

393   20.   K. Madhavan Nampoothiri, N. R. Nair and R. P. John, *Bioresource Technology*, 2010, **101**,
394   8493-8501.

395   21.   X. Wang, P. Qu and L. Zhang, *Fibers Polym*, 2014, **15**, 302-306.

396   22.   T. Serra, M. Ortiz-Hernandez, E. Engel, J. A. Planell and M. Navarro, *Materials Science and*
397   *Engineering: C*, 2014, **38**, 55-62.

398   23.   H. Li and M. A. Huneault, *Polymer*, 2007, **48**, 6855-6866.

399   24.   W.-C. Lai, W.-B. Liau and T.-T. Lin, *Polymer*, 2004, **45**, 3073-3080.

400   25.   J.-M. Yang, H.-L. Chen, J.-W. You and J. C. Hwang, *Polymer journal*, 1997, **29**, 657-662.

401   26.   H. Xu, L. Xie, X. Jiang, M. Hakkarainen, J.-B. Chen, G.-J. Zhong and Z.-M. Li,
402   *Biomacromolecules*, 2014, **15**, 1676-1686.

403   27.   H. Liu, W. Hu, Z. Zhang, L. Zhu and R. Ran, *Journal of Macromolecular Science, Part B*,
404   2014.

405   28.   M. W. Daniels, J. Sefcik, L. F. Francis and A. V. McCormick, *Journal of colloid and interface*
406   *science*, 1999, **219**, 351-356.

407   29.   M. Iijima, M. Tsukada and H. Kamiya, *Journal of colloid and interface science*, 2007, **307**,

408   418-424.
409   30.   X. Yin, Y. Tan, Y. Chen, Y. Song and Q. Zheng, *Polymer International*, 2012, **61**, 1439-1446.
410   31.   X. Yin, Y. Tan, Y. Gao, Y. Song and Q. Zheng, *Polymer*, 2012, **53**, 3968-3974.
411   32.   B. Kalb and A. Pennings, *Polymer*, 1980, **21**, 607-612.
412   33.   Y. Wen, H. Wu, S. Chen, Y. Lu, H. Shen and N. Jia, *Electrochimica Acta*, 2009, **54**,
413   7078-7084.
414   34.   B. Z. Tang and H. Xu, *Macromolecules*, 1999, **32**, 2569-2576.
415   35.   H. Roghani-Mamaqani, V. Haddadi-Asl, K. Khezri and M. Salami-Kalajahi, *Polymer*
416   *International*, 2014, **63**, 1912-1923.
417   36.   M. Amirian, A. N. Chakoli, J. H. Sui and W. Cai, *Polymer bulletin*, 2012, **68**, 1747-1763.
418   37.   C. S. Wu and H. T. Liao, *Journal of Polymer Science Part B: Polymer Physics*, 2003, **41**,
419   351-359.
420   38.   B. Zhao, H. Hu, A. Yu, D. Perea and R. C. Haddon, *Journal of the American Chemical Society*,
421   2005, **127**, 8197-8203.
422   39.   Y. Tan, L. Fang, J. Xiao, Y. Song and Q. Zheng, *Polymer Chemistry*, 2013, **4**, 2939-2944.
423   40.   M. Fang, K. Wang, H. Lu, Y. Yang and S. Nutt, *Journal of Materials Chemistry*, 2010, **20**,
424   1982-1992.
425   41.   Y.-Y. Liang, J.-Z. Xu, X.-Y. Liu, G.-J. Zhong and Z.-M. Li, *Polymer*, 2013, **54**, 6479-6488.
426   42.   S. Fujisawa, J. Zhang, T. Saito, T. Iwata and A. Isogai, *Polymer*, 2014, **55**, 2937-2942.
427   43.   S. Fujisawa, T. Saito, S. Kimura, T. Iwata and A. Isogai, *Biomacromolecules*, 2013, **14**,
428   1541-1546.
429   44.   M. Hikosaka, *Polymer*, 1987, **28**, 1257-1264.
430   45.   Y. He, Z. Fan, Y. Hu, T. Wu, J. Wei and S. Li, *European Polymer Journal*, 2007, **43**,
431   4431-4439.
432   46.   S.-Y. Lin, E.-C. Chen, K.-Y. Liu and T.-M. Wu, *Polymer Engineering & Science*, 2009, **49**,
433   2447-2453.
434   47.   M. Pracella, M. M.-U. Haque and D. Puglia, *Polymer*, 2014, **55**, 3720-3728.
435   48.   M. Cocca, M. L. D. Lorenzo, M. Malinconico and V. Frezza, *European Polymer Journal*,
436   2011, **47**, 1073-1080.
437
438